ENGINEERING AND INDUSTRIAL RESEARCH STATION

Quarterly Progress Report #9

NAS8-11334

RESEARCH STUDY FOR DETERMINATION OF LIQUID SURFACE PROFILE IN A CRYOGENIC TANK DURING GAS INJECTION

June 18, 1966 - September 17, 1966

COLLEGE OF ENGINEERING

MISSISSIPPI STATE UNIVERSITY

STATE COLLEGE, MISSISSIPPI

Engineering and Industrial Research Station
College of Engineering
Mississippi State University
P.O. Drawer PE, State College, Mississippi 39762

Quarterly Progress Report #9, NAS8-11334
RESEARCH STUDY FOR DETERMINATION OF LIQUID SURFACE PROFILE IN A CRYOGENIC TANK DURING GAS INJECTION

Period Covered: June 18, 1966 - September 17, 1966

Authors:

Dr. Wm. D. McCain, Jr.
Dr. E. H. Bishop
Mr. James T. Smith

Quarterly Progress Report
Contract Number: NAS8-11334
Control Number: DCN 1-4-50-01218-01 (1F)
CPB 02-1277-64

This report was prepared by Mississippi State University under NAS8-11334 RESEARCH STUDY FOR DETERMINATION OF LIQUID SURFACE PROFILE IN A CRYOGENIC TANK DURING GAS INJECTION, For the George C. Marshall Space Flight Center of the National Aeronautics and Space Administration. The work was administered under the technical direction of the Propulsion and Vehicle Engineering Laboratory, of the George C. Marshall Space Flight Center with Mr. Hugh M. Campbell acting as project manager.

TABLE OF CONTENTS

LIST OF FIGURES

LIST OF FIGURES -- continued

LIST OF TABLES

INTRODUCTION

This is the ninth Quarterly Progress Report for NAS8-11334, RESEARCH STUDY FOR DETERMINATION OF LIQUID SURFACE PROFILE IN A CRYOGENIC TANK DURING GAS INJECTION. The period covered is June 18, 1966 to September 17, 1966.

ANALYSIS OF PROGRESS

A larger bubble tank was constructed and tested this quarter. As the total gas flow rate was increased the surface waves in the previous eighteen-inch square tank splashed against the walls and obscured the view of the surface disturbance. A new tank five-feet square was constructed. Data in a flow rate region which overlaps that of previous data were obtained. The new data fit very closely to the previous correlations. Thus, it appears that the new tank can be used to extend the existing correlation.

The entrainment phase of this research during the past quarter was directed to a study of the influence of the entrapped-liquid viscosity on entrainment of the liquid by air streams. The same test sections utilized in the water tests are being used for the variable viscosity tests. From the limited data collected to date certain trends are indicated, however, additional tests are required before any definite conclusions may be drawn regarding the role of liquid viscosity in entrainment. Plots of entrainment versus time for various average air mass flow rates and liquid viscosities are presented and discussed in this report. These plots are explained in

terms of the liquid flow characteristics in various parts of the test section, and comparisons of these characteristics are made with those of water which are thoroughly described and discussed in Annual Report #2. The initial results indicate that at high air mass flow rates (greater than 6.66 lbm/min) for the viscosity range of 1cp-4cp changes in viscosity have very little effect upon entrainment. However, at low to medium (4.11 lbm/min to 6.66 lbm/min) air flow rates increases in viscosity cause significant reductions in entrainment.

PROGRESS

Surface Profile

The Second Annual Report, dated June 18, 1966, gives the height and shape of the surface profiles caused by rising swarms of gas bubbles as determined experimentally. The data cover an inlet gas flow rate of from 2 to 28 standard cubic feet per hour. Correlations of these data were also presented, which could be used to compute the shape of the disturbance for any inlet gas flow rate in that range. At the higher gas flow rates we began to experience difficulty in obtaining data in the 18-inch square tank then being used. Surface waves caused by the disturbance would splash against the sides of the tank obscuring the surface profiles. Consequently, it was determined that a larger tank would have to be built in order to permit extension of the inlet gas flow rate to higher rates.

The primary effort this quarter was devoted to designing, constructing and testing a larger bubble tank. The new tank is

five-feet square and approximately three feet in depth with the gas inlet device located in the center. We have again used a square tank for photographic considerations, and plexiglas was used as the material of construction. The first consideration was whether the data obtained using the new tank would agree with the previous data obtained with the smaller tank and would fit the previous correlations. Therefore, the first four surface profiles were obtained at gas flow rates between twelve and twenty-four standard cubic feet per hour, which fall within the range previously studied. Figures 1 through 6 show the four new data points along with the earlier data as presented in figures 46 through 51 of the Second Annual Report. It may be seen that the data obtained through use of the larger tank does fit well with the earlier data. The addition of this data, presented in Table 1, has not changed the generalized non-dimensional surface disturbance shape, which was presented as Figure 44 in the Second Annual Report, and is repeated here as Figure 7. Figures 8 through 11 give comparisons of the new data with the correlations given in Figures 7, 1, and 6.

Entrainment

The primary effort during this report period was devoted to initiating a study of the influence of the viscosity of an entrapped liquid on the removal of this liquid by an air stream.

Viscosity variation was accomplished by using various mixtures of glycerine and water. Since the viscosity of glycerine is temperature dependent and since the air stream temperature often varies from 10° to 15°F in the course of a day's operation, which in turn causes the

Table 1. Experimental Surface Profiles Obtained Through Use of the Five Foot Square Bubble Tank. Distilled Water Nitrogen System.

Inlet Gas Flow Rate-Standard Cubic Feet Per Hour	Average Surface Profile Data, feet					Number of Surface Disturbances Analyzed to Yield Average Surface Profile Data
	Z_m	$Z_{r=0}$	$Z_{r=0.25}$	$Z_{r=0.50}$	$Z_{r=0.75}$	
12.36	0.0684	0.0583	0.0526	0.0436	0.0291	60
19.55	0.0758	0.0592	0.0561	0.0437	0.0263	60
21.55	0.1012	0.0825	0.0753	0.0625	0.0378	59
23.70	0.0994	0.0828	0.0722	0.0594	0.0374	60

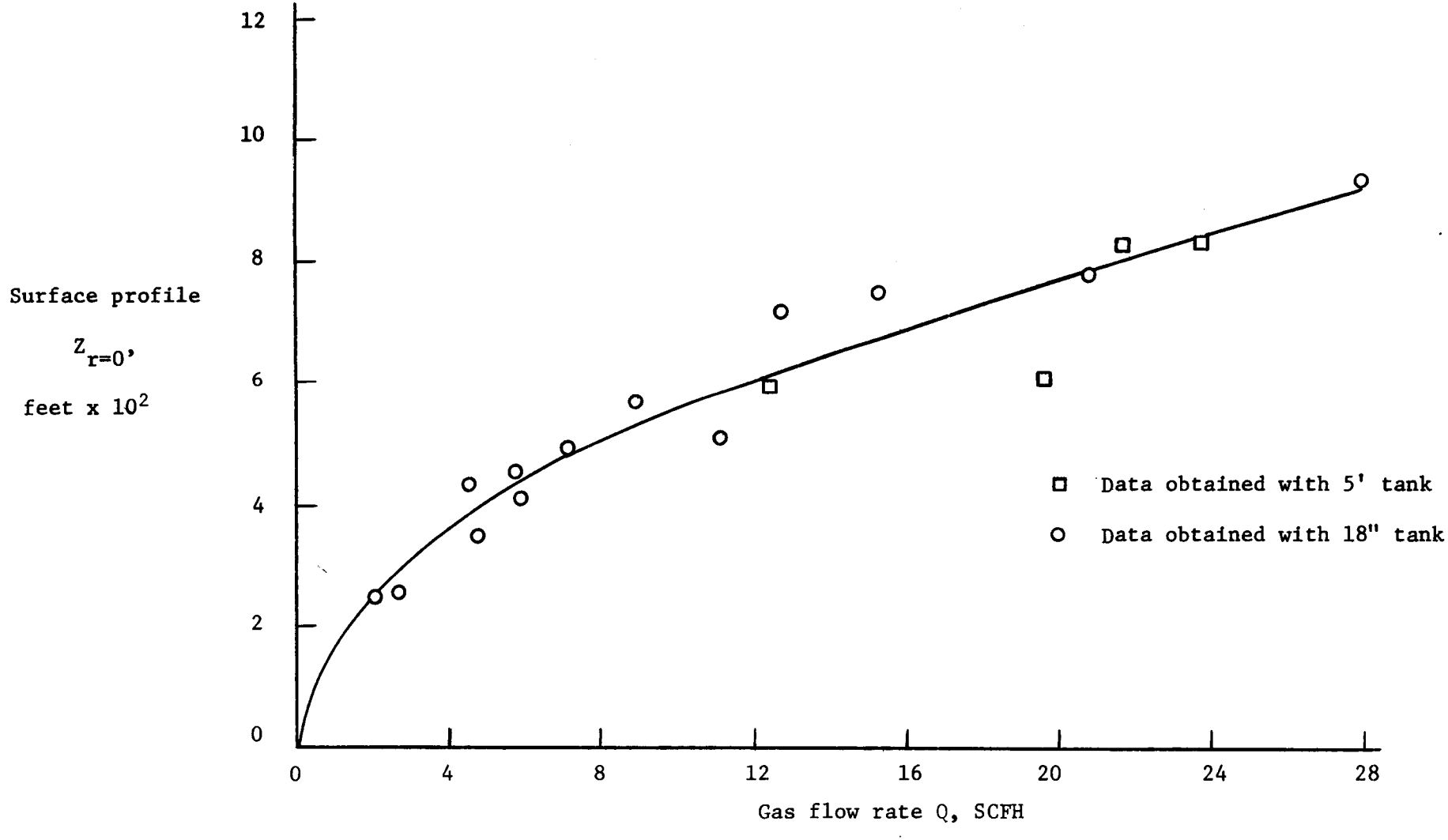

Figure 1. Comparison of Surface Profile Data for the 18" and 5' Bubble Tanks at a Dimensionless Radial Coordinate, r = 0.0. Nitrogen Gas in Distilled Water.

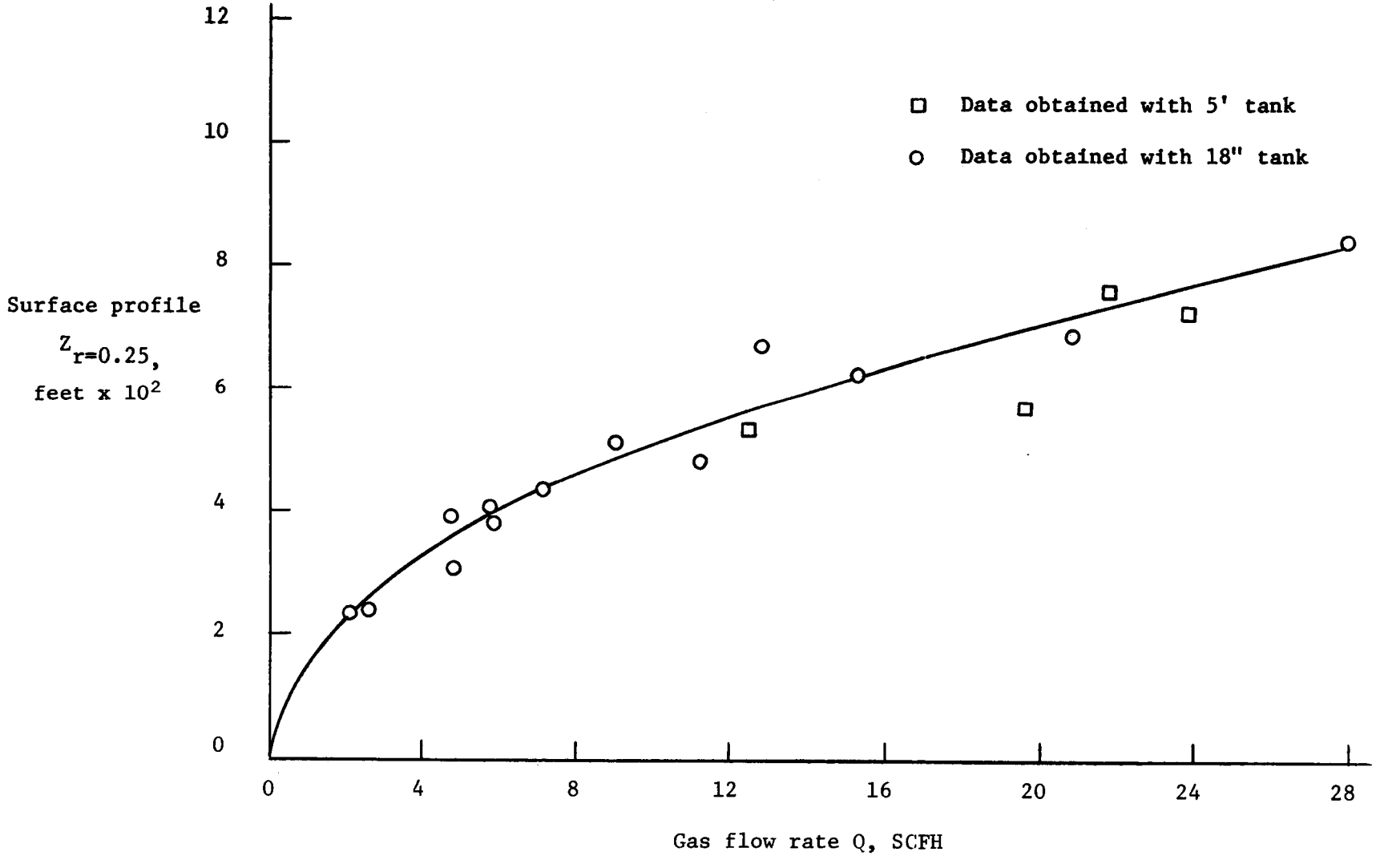

Figure 2. Comparison of Surface Profile Data for the 18" and 5' Bubble Tanks at a Dimensionless Radial Coordinate, $\bar{r}$ = 0.25. Nitrogen Gas in Distilled Water.

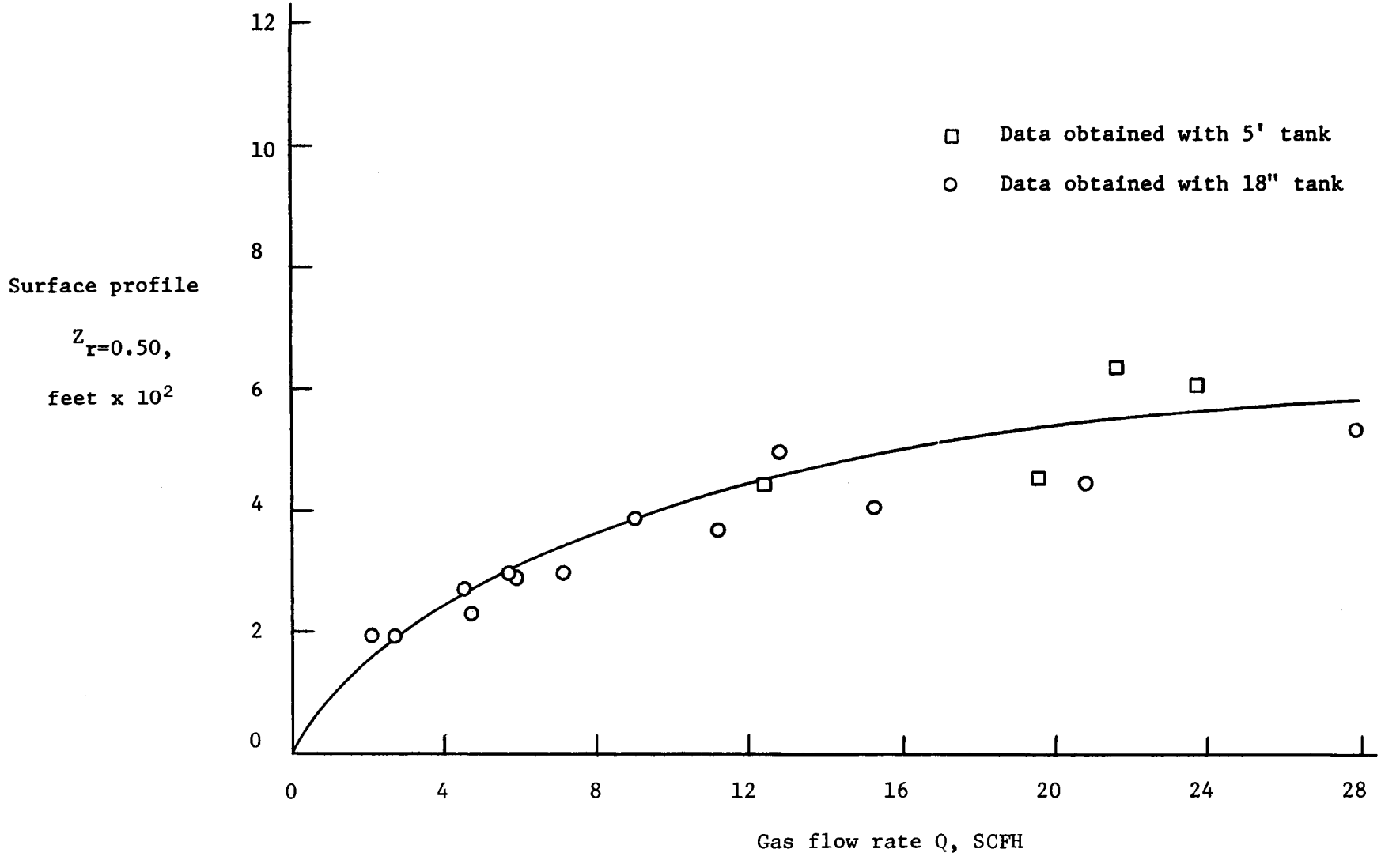

Figure 3. Comparison of Surface Profile Data for the 18" and 5' Bubble Tanks at a Dimensionless Radial Coordinate, r = 0.50. Nitrogen Gas in Distilled Water.

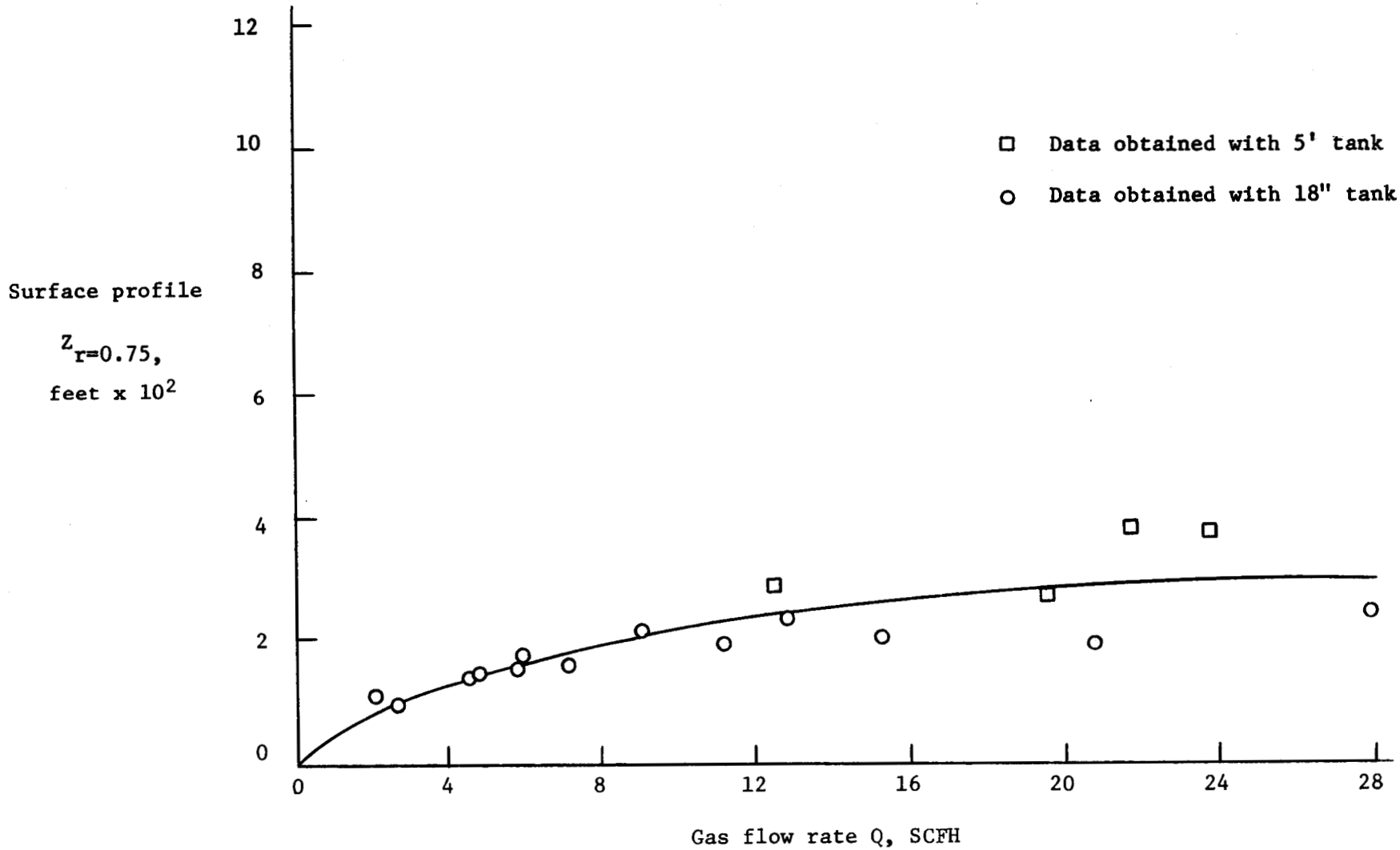

Figure 4. Comparison of Surface Profile Data for the 18" and 5' Bubble Tanks at a Dimensionless Radial Coordinate, r = 0.75. Nitrogen Gas in Distilled Water.

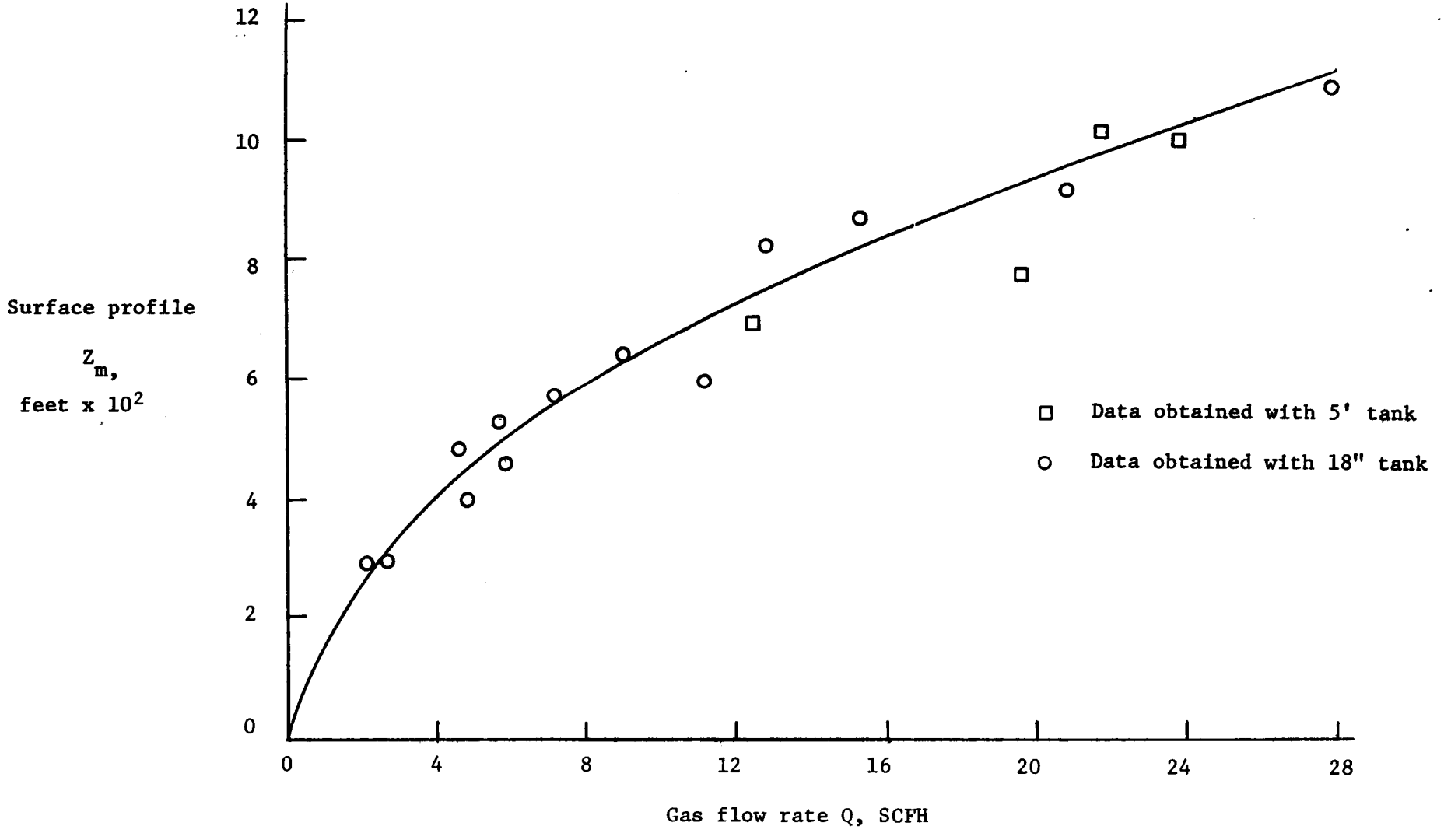

Figure 5. Comparison of Maximum Surface Profile for the 5' and 18" Tanks. Nitrogen Gas in Distilled Water.

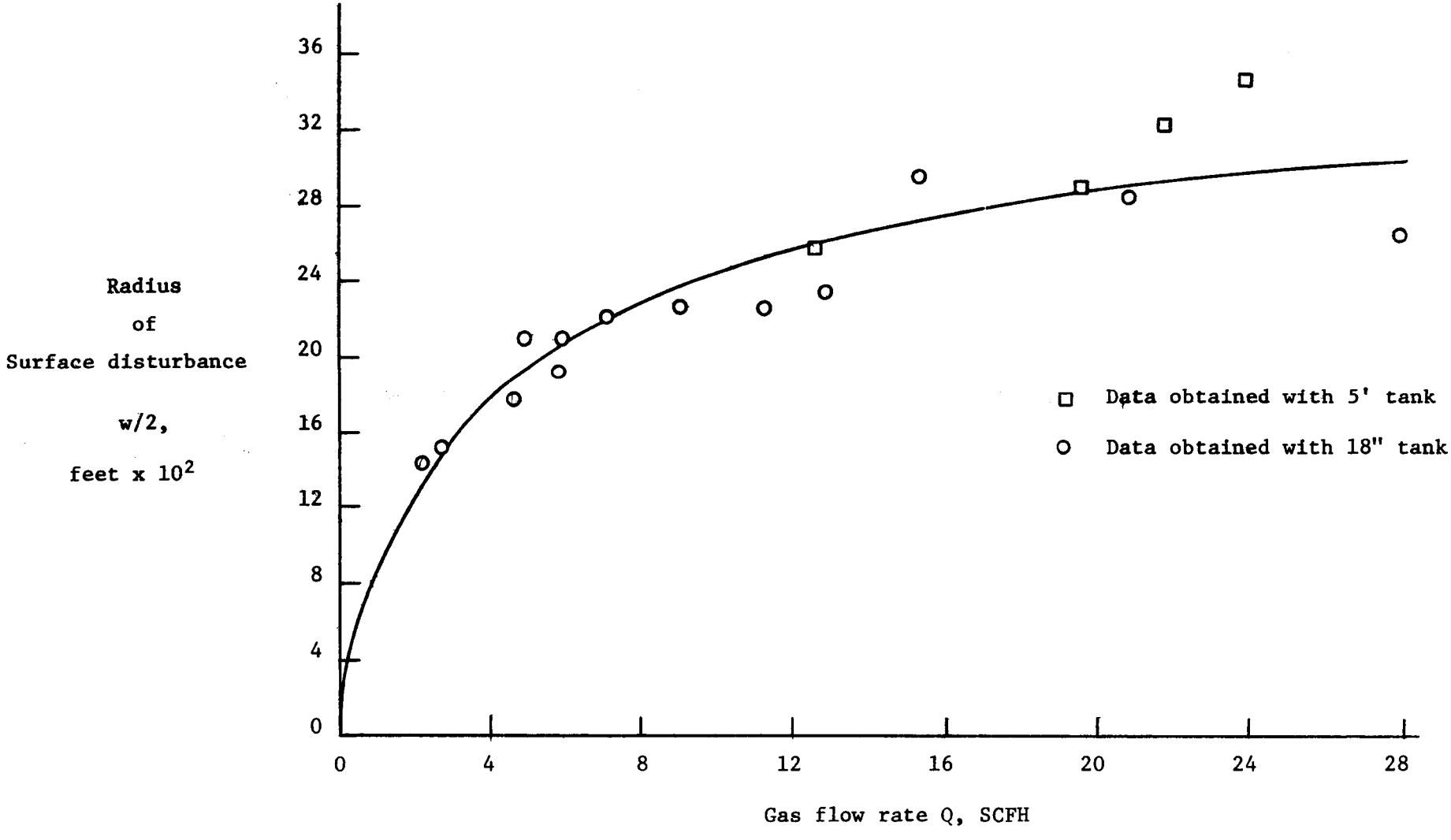

Figure 6. Comparison of Surface Profile Width Data for the 5' and 18" Tanks. Nitrogen Gas in Distilled Water.

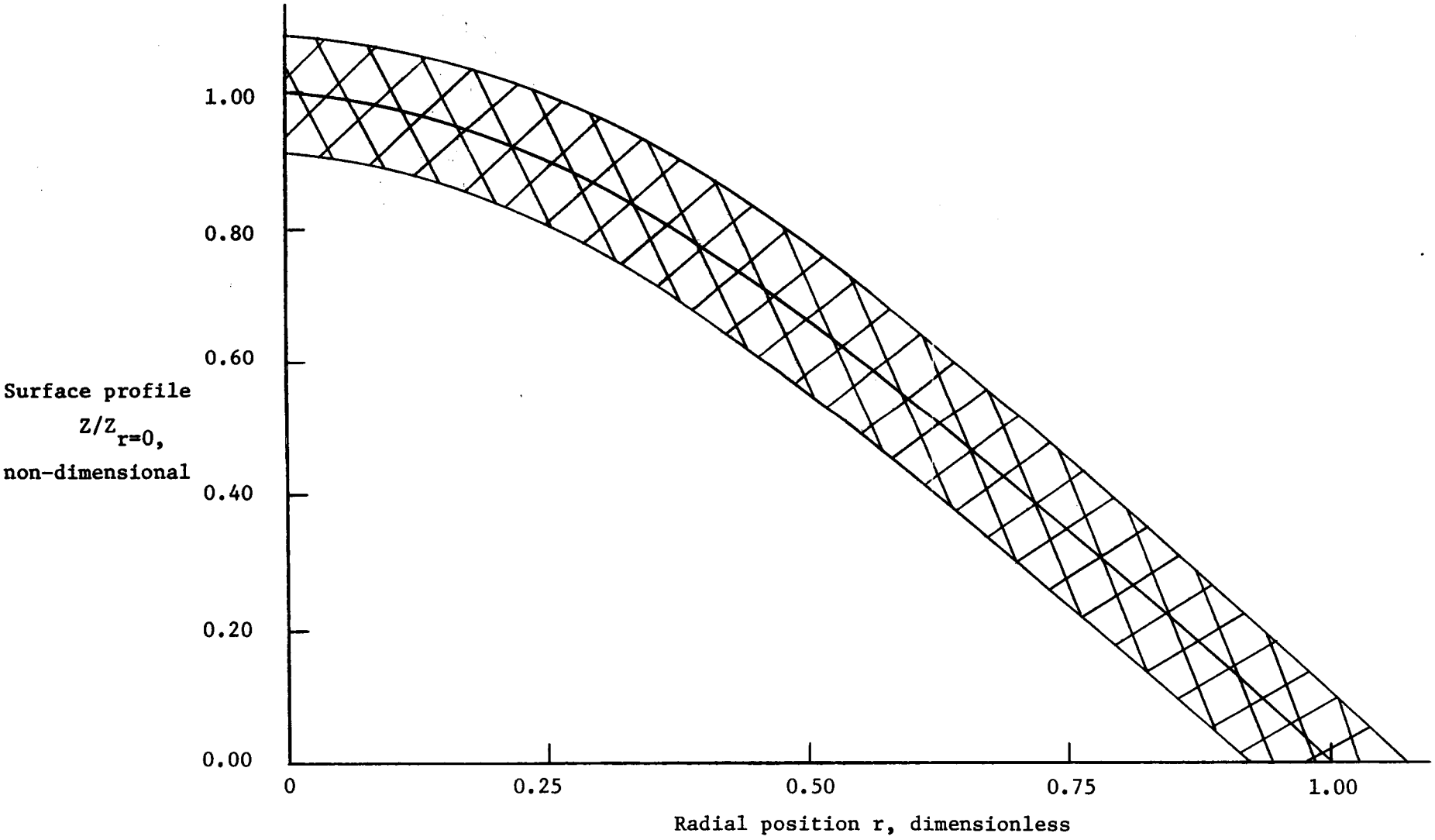

Figure 7. Non-dimensional Surface Profile $Z/Z_{r=0}$, versus Dimensionless Radial Coordinate r, for the Distilled Water-Nitrogen System.

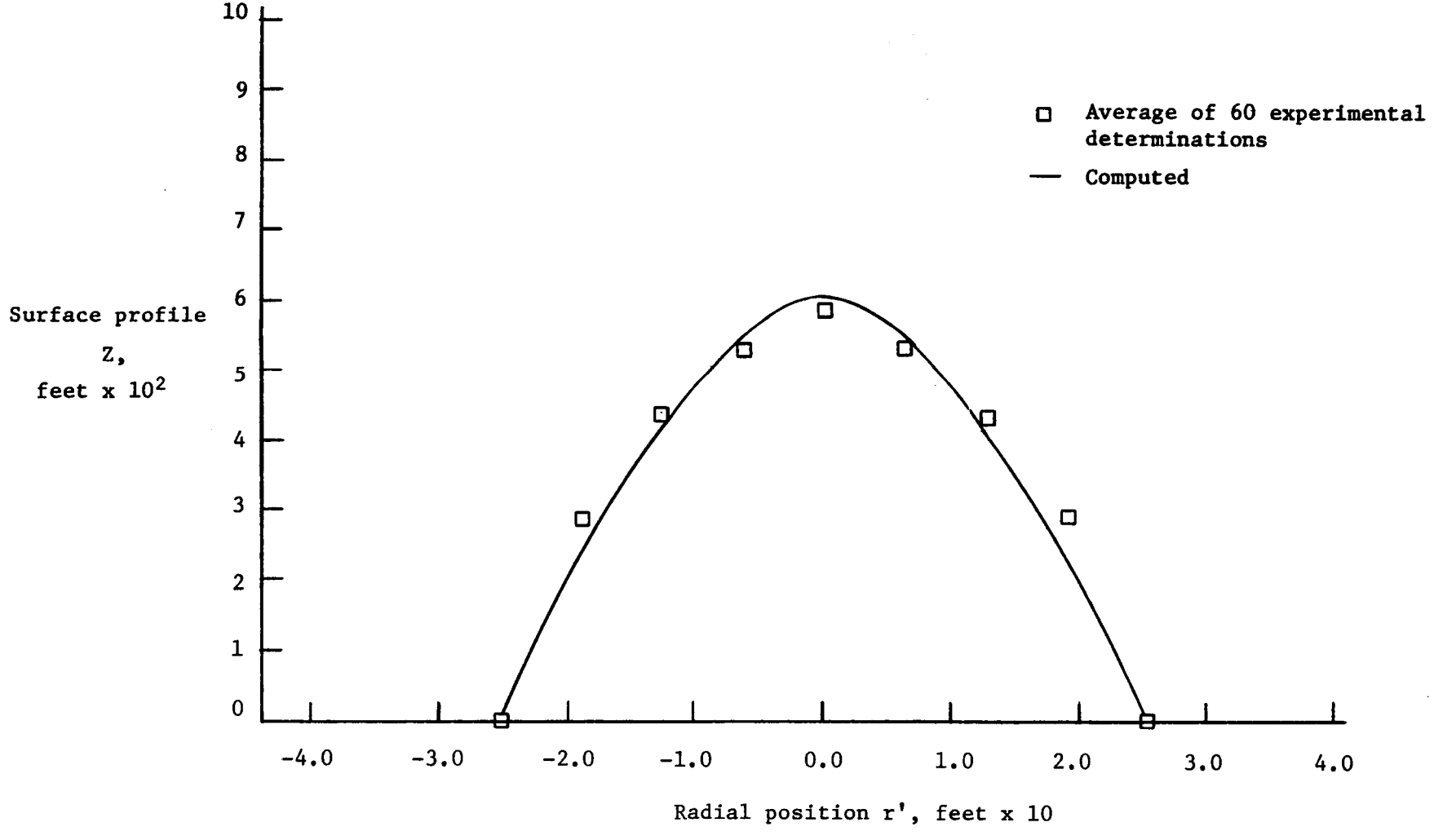

Figure 8. Comparison of Surface Profile Correlation with the Experimental Profile in Water Caused by a Rising Swarm of Nitrogen Bubbles at an Overall Inlet Gas Flow Rate of 12.36 Standard Cubic Feet Per Hour from a Square Configuration of Nine Hypodermic Needles.

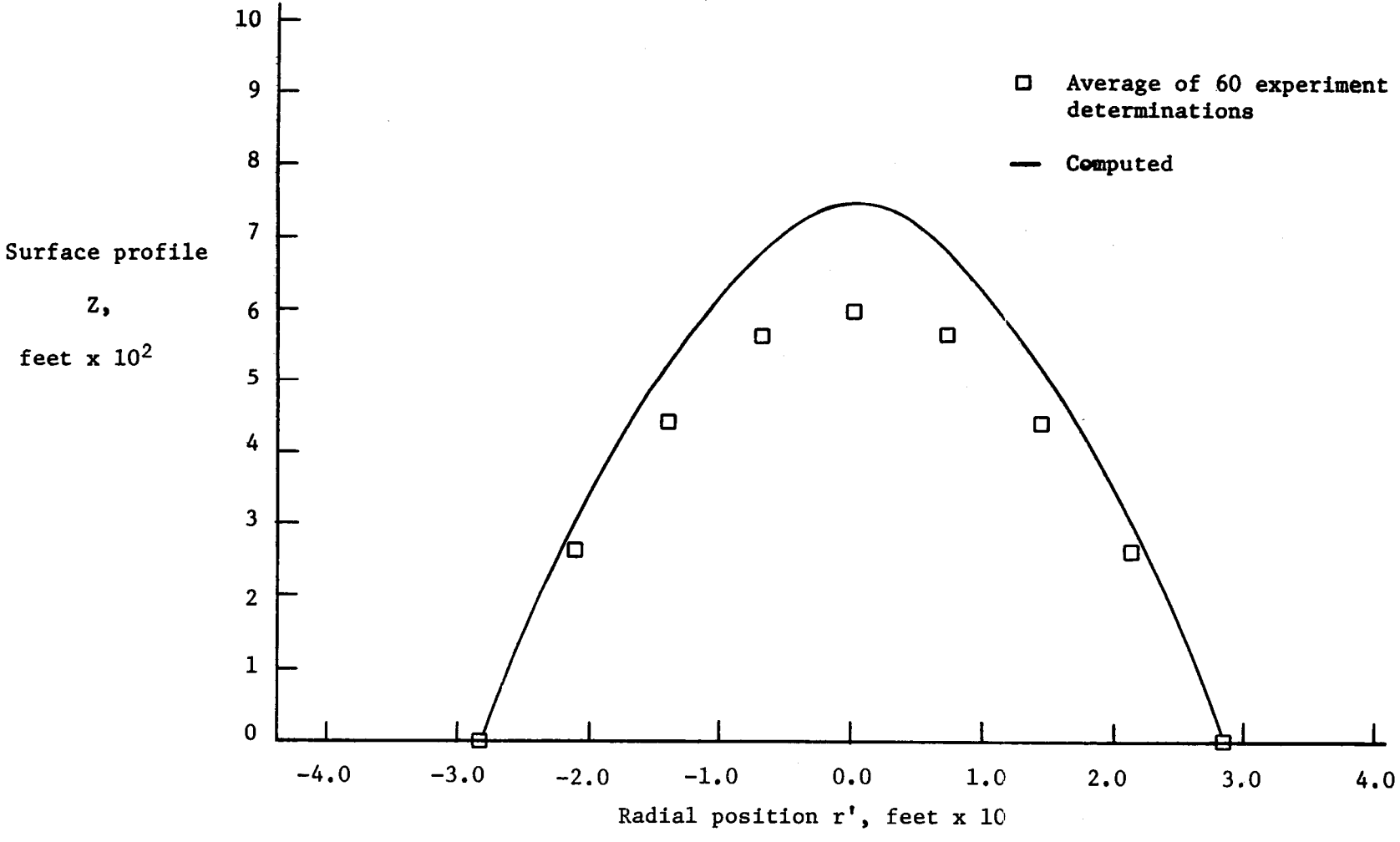

Figure 9. Comparison of Surface Profile Correlation with the Experimental Profile in Water Caused by a Rising Swarm of Nitrogen Bubbles at an Overall Inlet Gas Flow Rate of 19.55 Standard Cubic Feet Per Hour from a Square Configuration of Nine Hypodermic Needles.

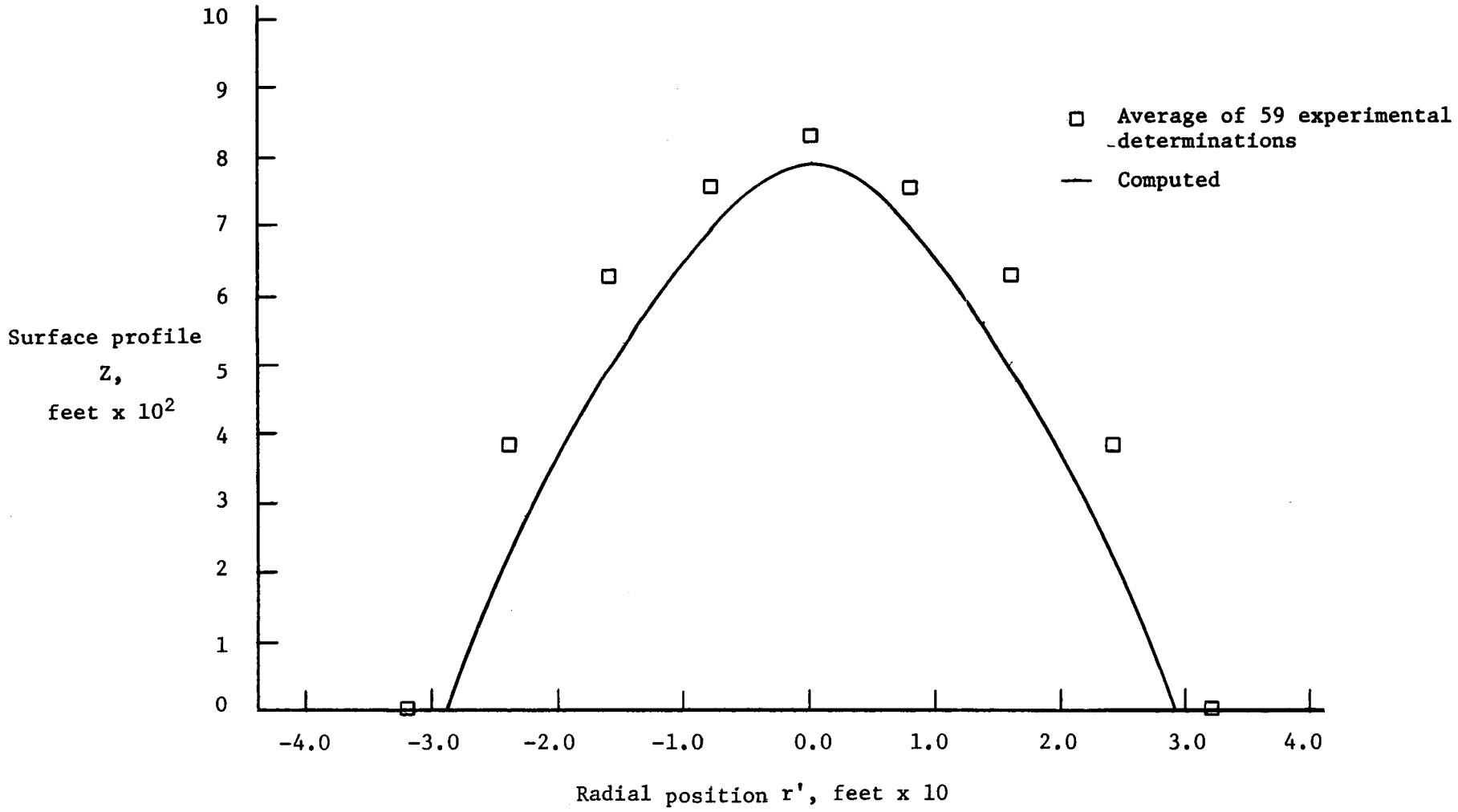

Figure 10. Comparison of Surface Profile Correlation with the Experimental Profile in Water Caused by a Rising Swarm of Nitrogen Bubbles at an Overall Inlet Gas Flow Rate of 21.55 Standard Cubic Feet Per Hour from a Square Configuration of Nine Hypodermic Needles.

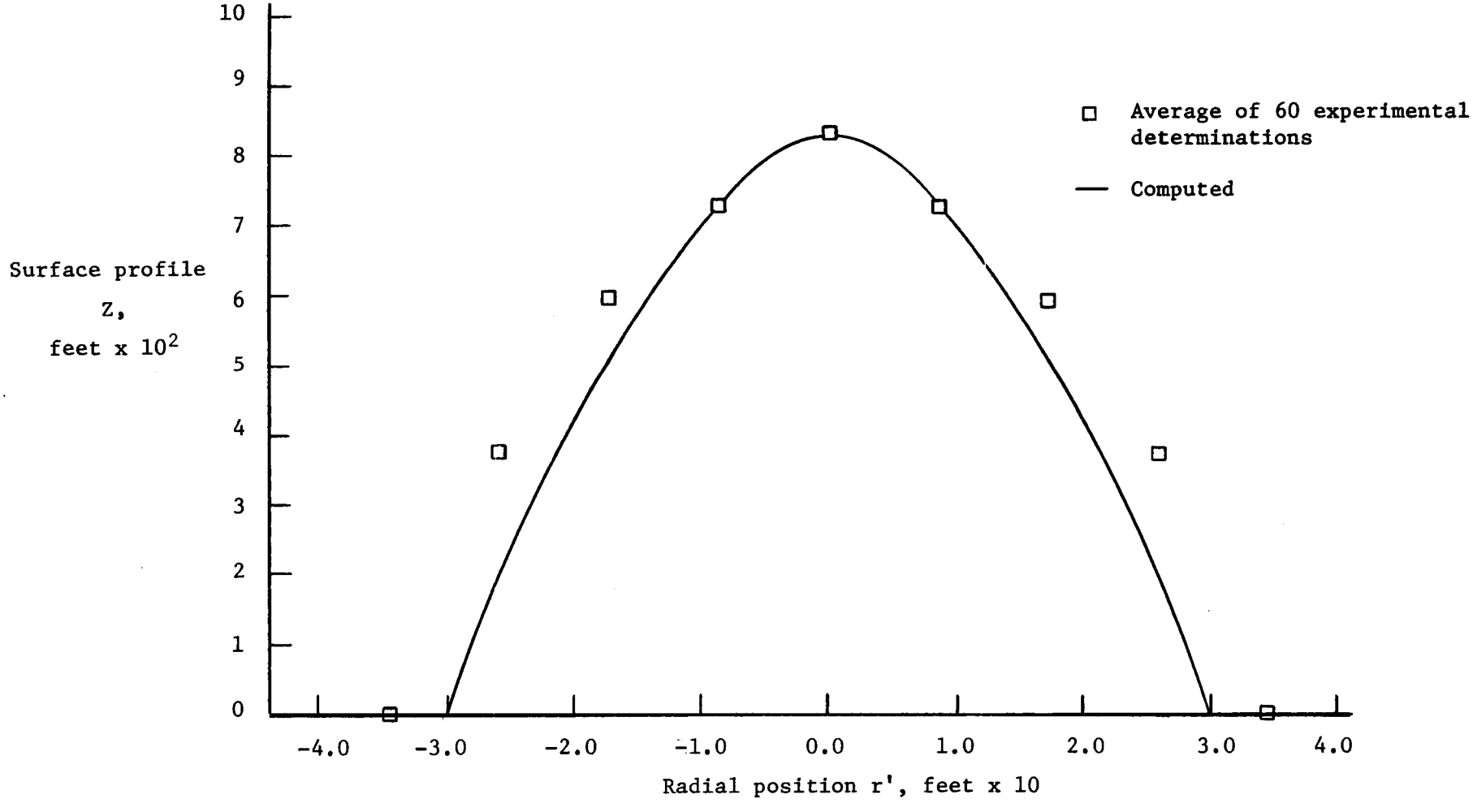

Figure 11, Comparison of Surface Profile Correlation with the Experimental Profile in Water Caused by a Rising Swarm of Nitrogen Bubbles at an Overall Inlet Gas Flow Rate of 23.70 Standard Cubic Feet Per Hour from a Square Configuration of Nine Hypodermic Needles.

glycerine-water mixture temperature to vary, the viscosity of the mixture was measured several times during the course of a run and averaged. In every instance where a viscosity value is quoted, e.g., on curves of entrainment versus time, it represents an average value.

Since only a limited range of viscosity values has been investigated to date, the results to be presented are not conclusive, however, certain trends are indicated. It should be pointed out that the amount of time required to complete a run at a given average air mass flow rate has now doubled that required for the water test.

The geometrical configurations previously studied using water as the confined liquid are being used for this investigation so that geometrical influences on the entrainment will be the same for both series of tests. The geometrical configuration presently being tested is shown in figure 12. Also, the same upstream-air static pressures used in the water tests are being used in the variable viscosity test, however, for a given upstream air pressure the average mass flow rates are different for the two series of tests; the mass flow rate for the variable viscosity test being slightly higher. This results from the changes made to the entrained-liquid carry-out system to reclaim the glycerine-water mixture; the pressure loss now being actually less than in the water system.

Flow Characteristics

For glycerine-water mixtures with viscosities up to approximately 50% greater than that of water at standard temperature (viscosity approximately one centipoise), no appreciable changes to the liquid flow

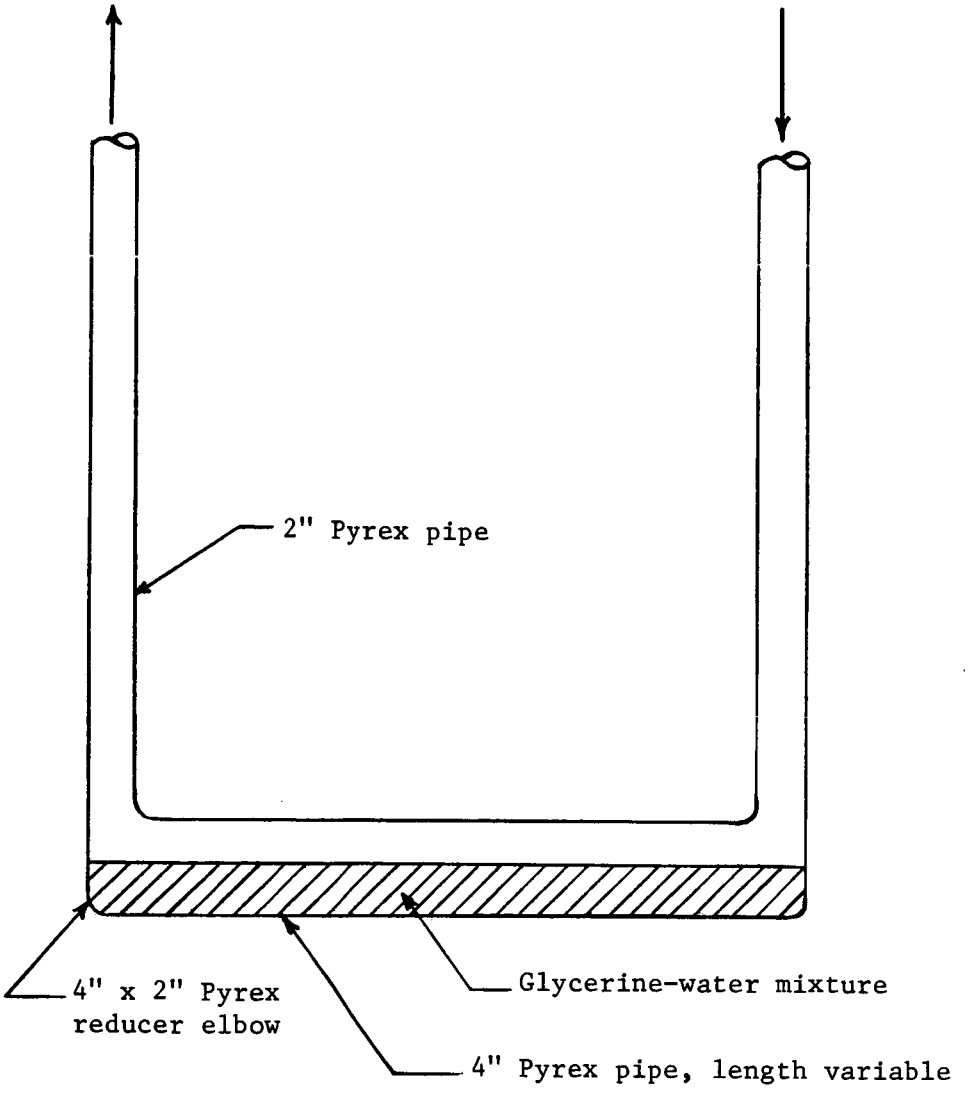

Figure 12. Entrainment Test Section

characteristics previously reported for water in the horizontal part of the test section shown in figure 12 could be observed. The different zones of flow defined in Annual Report #2 qualitatively describe the flow phenomena observed in the present series of tests. However, for a glycerine-water mixture with a viscosity of approximately four centipoise the wavelength and amplitude of the waves in zone 3 were considerably less than in the water tests for approximately the same average mass flow rate of air. Other characteristics of the flow were identical, with an apparent increase in mist formation at the downstream end of zone 3 where the waves impinge on the 90° elbow joining the horizontal pipe to the vertical pipe. (This is likely the result of a decrease in the surface tension.) The major means by which the glycerine-water mixture is transported from the test section is by this wave impingement which splashes liquid up into the vertical pipe forming both a fine mist and a thin film which is carried by the air up the vertical pipe. Visual observation of the flow in the vertical pipe indicates that the wetability of the glycerine-water mixture is greater than that of the water; the film covers a larger percentage of the surface of the vertical pipe than for water at small average mass flow rates of air.

The flow in the vertical pipe for the glycerine-water mixtures investigated to date, viscosities of from 1cp to 4cp, is similar to that described and shown in figure 11 of Annual Report #2. For a mixture with a viscosity of approximately 4 cp there was an apparent increase in the amount of mist being carried up the vertical pipe. The mist was not formed by liquid in the film falling back into the

horizontal pipe, as in the water tests, but by the impingement of waves on the downstream 90° elbow. Some frothing was observed periodically which resulted in an increase in mist formation.

Entrainment Rates

Figures 13 and 14 are plots of entrainment E versus time t for entrapped liquid quantities of 1/4 and 1/2 of the total volume of the horizontal pipe of the test section; the curves are for a given average mass flow rate and liquid viscosity. (The data are presented in Appendix I.) It is obvious upon a quick inspection of these plots that nearly all of the curves are for a different value of the viscosity. This results from the sharp dependence of the viscosity of glycerine upon temperature, and the fact that the temperature of the glycerine-water mixture varies during the course of a day's operation. The above points were discussed previously. The entrainment curves for water are not shown in figures 13 and 14 since the average air mass flow rates differ by as much as 4 lbm/min from those for the glycerine-water test for the same upstream air static pressure. The reason for this flow rate difference has been explained.

For the 1/2 filled case, figure 13, the data is limited to the viscosity range 1.19 cp to 1.364 cp with only one value of the viscosity for each of the average air mass flow rates of 12.55 lbm/min and 9.96 lbm/min. For air mass flow rates of 6.66 lbm/min and 4.11 lbm/min two viscosity curves are shown in figure 13 for each flow rate (the viscosities differ by approximately 9%). In each case an increase in the viscosity caused a reduction in the entrainment at all times. At the

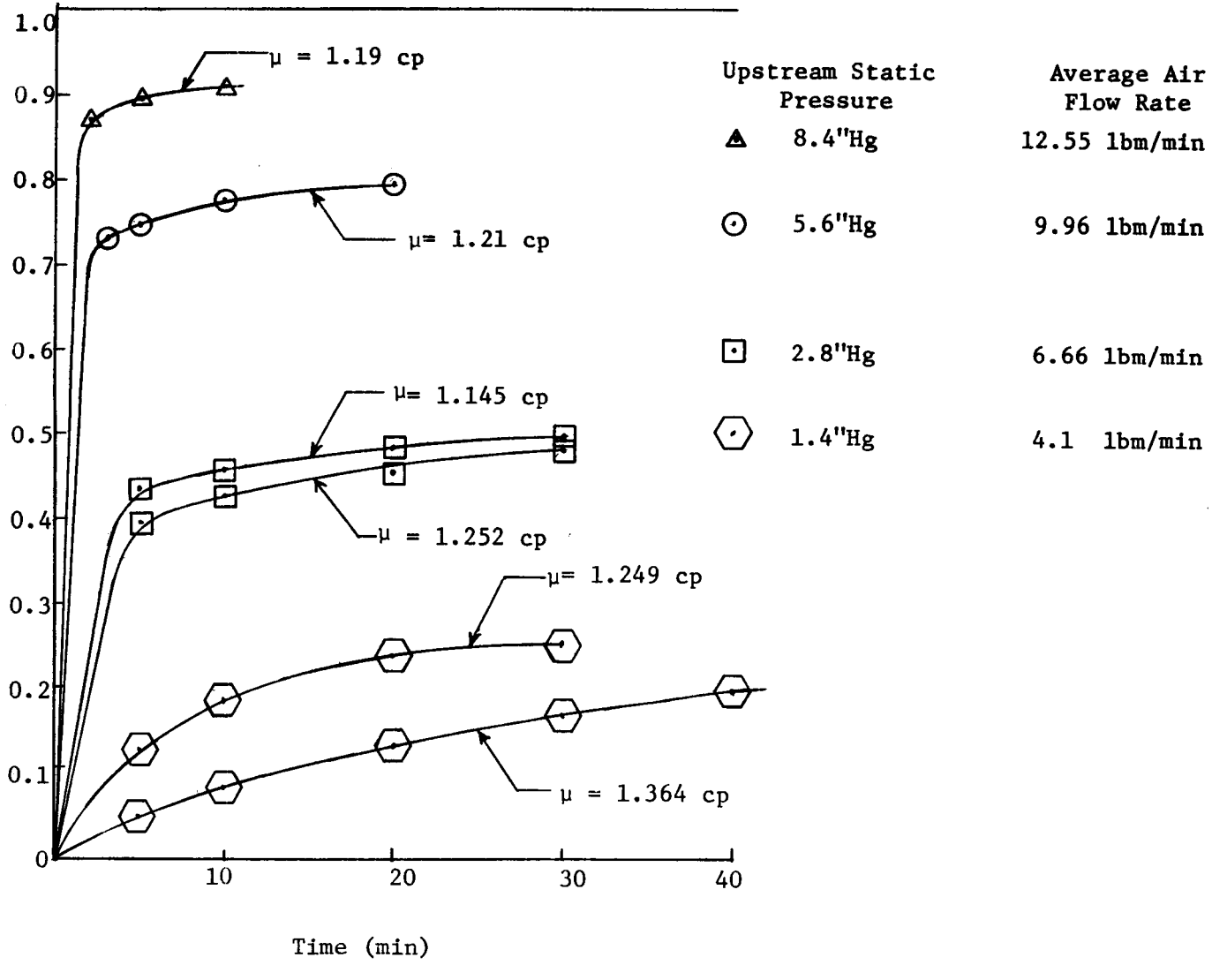

Figure 15. Entrainment versus Time for the Configuration Shown in Figure 12 (1/2 Filled, 5-Foot Horizontal Pipe) For Various Air Flow Rates and Viscosities.

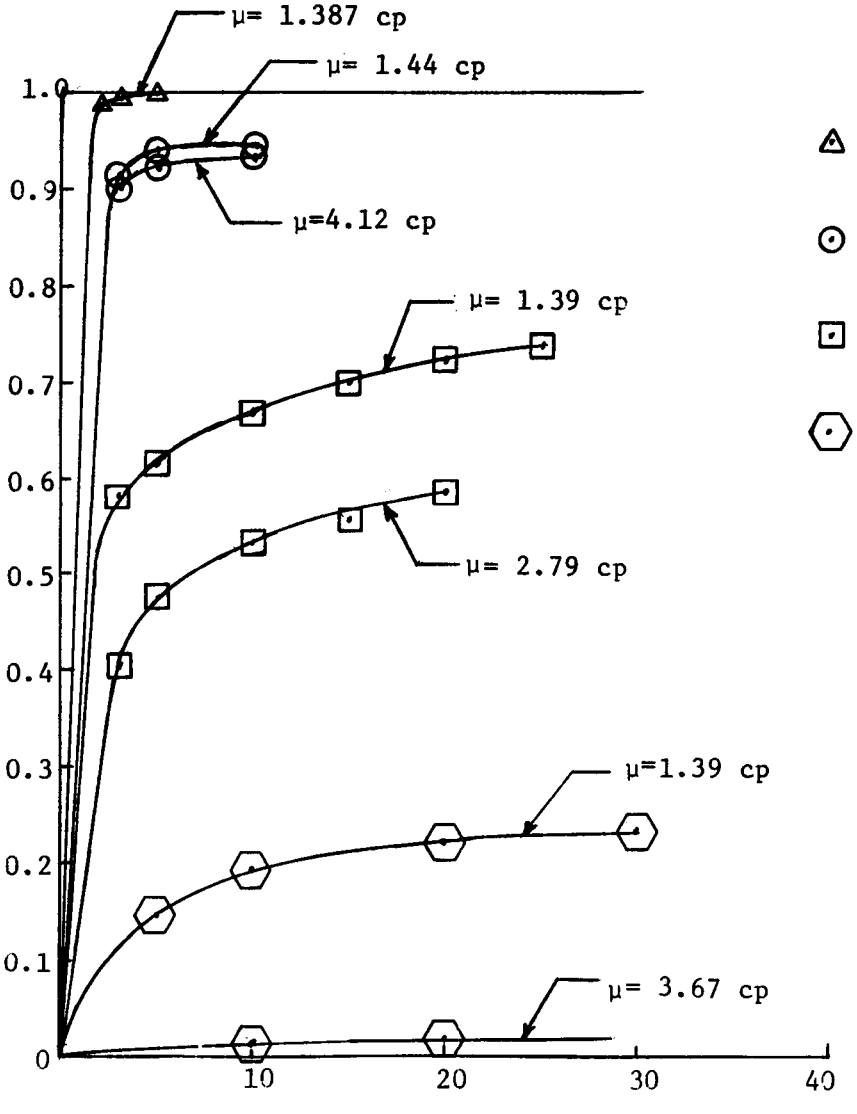

	Upstream Static Pressure	Average Air Flow Rate
△	19.2"Hg	21.26 lbm/min
⊙	12.8"Hg	16.29 lbm/min
⊡	6.4"Hg	10.86 lbm/min
⬡	3.2"Hg	7.55 lbm/min

Figure 14. Entrainment versus Time for the Configuration Shown in Figure 12 (1/4 Filled, 5-Foot Horizontal Pipe) for Various Air Flow Rates and Viscosities.

lower mass flow rate the reduction in entrainment was the greatest; as much as 57% at t=10 min., however, as t increases the total reduction is approximately 23%. It appears that small changes to the viscosity will have negligible effect upon entrainment at the higher (greater than 6.66 lbm/min) flow rates. Additional data in this area is required. The reductions in entrainment found as the viscosity of the liquid was increased may be attributed primarily to the increased frictional loss of the film in the vertical pipe; of secondary importance is the increase in mist formation and removal of liquid as fine droplets entrained in the air, the sum of the two "entrainment-reducing" effects, increased frictional loss and specific gravity, outweighs this "entrainment-increasing" effect.

For the 1/4-filled case, figure 14, several viscosity curves are shown for each average air mass flow rate. For the higher air flow rates, 17 lbm/min to 22 lbm/min, increases in viscosity of around 360% did not materially affect the entrainment, though there was some reduction. At these higher flow rates a majority of the liquid is removed initially in large slugs. Since the specific gravity of the glycerine-water mixtures tested did not exceed 1.13 and since viscosity does not materially effect slug flow (the gravity force being predominate in the particular geometry of this research) there should be little effect upon the entrainment at these flow rates as the viscosity is increased to approximately 4 cp with a corresponding specific gravity of 1.13. For lower flow rates, 10.8 to 7.5 lbm/min., the entrainment curves for a viscosity of approximately 4 cp are considerably below those for a viscosity of 1.39 cp. Since the

removal of the liquid from the test section at these flow rates is predominately by the flowing film, viscosity changes have more effect on the entrainment.

CURRENT PROBLEMS

Surface Profile

Now that the larger tank is in use, the previous problems in obtaining unobscured motion picture recordings of the surface disturbances have been eliminated and there are no problems delaying the work at this time.

Entrainment

There are no problems delaying the work on the entrainment phase of the research at this time.

PLANS FOR NEXT QUARTER

Surface Profile

The correlations given in Figures 1 through 7 will be extended into the higher inlet gas flow rate regime through analysis of motion picture recordings made using the new large bubble tank.

Entrainment

The variable viscosity tests will be continued, to be terminated with tests for pure glycerine.

APPENDIX I

ENTRAINMENT DATA

Table II. Entrainment Versus Time for Test Section Shown in Figure 12 (1/4 - Filled) for Various Air Flow Rates and Liquid Viscosities

Time Min.	Upstream Air Pressure Inches Hg	Average Mass Flow Rate of Dry Air lbm/min	Average Liquid Viscosity Centipoise	Entrainment
0-5	3.2	7.575	1.39	0.1485
0-10		7.555		0.193
0-20		7.530		0.222
0-30		7.530		0.232
0-10	3.2	7.250	3.67	0.0125
0-3	6.4	10.890	1.39	0.582
0-5		10.905		0.619
0-10		10.815		0.670
0-15		10.770		0.70
0-20		10.940		0.729
0-25		10.840		0.740
0-3	6.4	11.04	2.79	0.406
0-5		11.00		0.478
0-10		11.035		0.533
0-15		11.035		0.557
0-20		10.97		0.588
0-3	12.8	16.275	1.44	0.916
0-5		16.320		0.946
0-10		16.205		0.947
0-2	12.8	16.203	4.12	0.904
0-3		16.17		0.91
0-5		16.23		0.925
0-10		16.22		0.931
0-2	19.2	21.235	1.387	0.986
0-3		21.380		0.994
0-5		21.260		0.993
0-2	19.2	21.28	3.65	0.988
0-3		21.32		0.996
0-5		21.265		0.996

Table III. Entrainment Versus Time for Test Section Shown in Figure 12 (1/2-Filled) for Various Air Flow Rates and Liquid Viscosities

Time Min	Upstream Air Pressure Inches Hg	Average Mass Flow Rate of Dry Air lbm/min	Average Liquid Viscosity Centiposie	Entrainment
0-5	1.4	4.185	1.249	0.126
0-10		4.055		0.185
0-20		4.020		0.236
0-30		4.040		0.252
0-5	1.4	4.235	1.364	0.049
0-10		4.195		0.082
0-20		4.145		0.132
0-30		4.160		0.168
0-40		4.040		0.195
0-5	2.8	6.600	1.145	0.433
0-10		6.515		0.457
0-20		6.615		0.484
0-30		6.705		0.496
0-5	2.8	6.700	1.252	0.397
0-10		6.765		0.428
0-20		6.715		0.457
0-30		6.635		0.480
0-3	5.6	9.910	1.210	0.734
0-5		9.985		0.745
0-10		10.045		0.778
0-20		9.920		0.792
0-3	5.6	10.020	1.269	0.734
0-5		9.990		0.737
0-10		10.055		0.755
0-2	8.4	12.555	1.190	0.871
0-5		12.485		0.895
0-10		12.605		0.907